Appl. Math. Inf. Sci. 6, No. 1, 89-98 (2012)

Applied Mathematics & Information Sciences

An International Journal

@ 2012 NSP
Natural Sciences Publishing Cor.

Design of Dynamic Sliding Mode Controller to Aeroelastic Systems

Chieh-Li Chen[1], Chung-Wei Chang[1] and Her-Terng Yau[2]

[1]*Department of Aeronautics and Astronautics, National Cheng Kung University, Tainan, Taiwan*
[2]*Department of Electrical Engineering, National Chin-Yi University of Technology, Taichung, Taiwan*

Received: Received May 02, 2010; Revised July 25, 2011; Accepted September 12, 2011
Published online: 1 January 2012

Abstract: It is well known that for the model with a single trailing-edge control surface, trajectory control of either the plunge displacement or the pitch angle (but not of both) can be achieve by the controller design and there exist internal dynamics describing the residual motion in aeroelastic closed-loop systems. The internal dynamics of aeroelastic depend on the model parameters including the free stream velocity and spring constant. Motivated by the limited effectives of using single control surface, improvements in control of limit-cycle oscillation by using leading- and trailing-edge control surface are investigated. Moreover, two control surfaces provide flexibility in shaping both the plunge and the pitch responses. This study uses the dynamic sliding mode control (DSMC) to achieve system stability and eliminate the phenomenon of limit cycle response. Compared to the conventional sliding mode control design, the proposed control law preserves not only the robustness of the system but also avoids chattering phenomenon. Simulation results are presented which show that these controllers are effective in regulating the response to origin in state space in spite of controller input with saturation.

Keywords: Aeroelastic system, Limit cycle oscillation, Dynamic sliding mode control.

1. Introduction

The aeroelastic system contains the nonlinear interactions generated by structure, inertial force and aerodynamics, which can lead to unsteady phenomena such as flutter and limit cycle oscillation, and result in unstable effects to aircrafts. When a dynamic system consists of nonlinear behaviors, system trajectory tends to be in some specific states called 'the attractors' of the system. The common attractors are dots that mostly appeared in some state points or circulate on 'the rings' that composed by a group of system states. This type of 'dots' or 'rings' can be named as the 'fixed points' or the 'limit cycle oscillations, respectively. The reason why limit cycle oscillations would occur in the aeroelastic system is yet not apparent, but it is most believed that the effect of structural nonlinearity and aerodynamics is the major cause of such phenomenon. This infers that the nonlinearity in the structural spring constant leading to limit cycle oscillations can be proved by testing its system stiffness. If the limit cycle oscillations constantly occur in the aeroelastic system, the aircraft wing structure will suffer continuing impairment, even worst, bring about catastrophic consequences to the aircraft. Therefore, to provide a practical controller to eliminate such flutter and limit cycle oscillation phenomena is one of the important tasks in the aircraft industry.

The dynamics of an aeroelastic system varies with the external force exerted, which is lift and moment, due to the aerofoil with the influence of the pitch angle and the plunge displacement. A wealth of effort had been put into the dynamic analysis either by numeric analysis or experiments. Recently, many researchers have been done to investigate and analysis aeroelastic dynamics [1-7]. It shows that the dynamic behavior of aeroelastic system is very complex. Other than the study on the issue of system dynamics, the design of a

[2]Corresponding author. *pan1012@ms52.hinet.net*

control law as a way to prohibit flutter is as well a major concern in an aeroelastic system. Among the prior works, there had been a great number of relevant control law designs, in which the system is modeled as the one merely with a trailing edge control input such as nonlinear adaptive control [8], feedback linearization [9], and adaptive feedback linearization [10], adaptive neural network approach [11], among many others [12-15].

Sliding mode control (SMC) [16] provides an effective alternative to deal with uncertain chaotic systems, and has been successfully applied in controlling nonlinear system [17]. In the traditional SMC, it is assumed that the control can be switched from one value to another infinite fast, and this is impossible due to finite time delays and limitations in practical system. This non-ideal switching result in an undesirable phenomenon called chattering. The boundary layer approach is introduced to eliminate chattering around the switching surface and the control discontinuity within this thin boundary layer is smoothed out. If systems uncertainties are large, the sliding mode controller would require a high switching gain with a thicker boundary layer to eliminate the higher chattering effect resulting. However, if we continuously increase the boundary layer thickness, we are actually reducing the feedback system to a system without sliding mode. To tackle these difficulties, a dynamic sliding mode control (DSMC) is applied to deal with the chattering phenomenon. The approach is one of the most popular nonlinear techniques of control design. DSMC has received attention in recent years [18-19]. Introducing extra dynamics into a sliding surface helps to solve many difficulties in practice, such as flight control design and timescale separation of control loops in a multi-loop system.

In this work, a control strategy for aeroelastic systems that addresses unsteady phenomenon, such as flutter and limit cycle oscillation suppression problem is developed. The proposed strategy is an input-output control scheme which comprises two sliding mode controllers and two integrators. Based on this proposed method, the dynamic sliding mode control concept is used to obtain a continuous control input. Simulation results show that the proposed controller can eliminate the flutter undergone in an aeroelastic system, with a continuous control input.

2. Aeroelastic systems modeling

Illustrated in Fig. 2.1 is an aeroelastic system model where the wing is of two freedoms. The dynamic equation of an aeroelastic system can be expressed as [20]

$$\begin{bmatrix} I_\alpha & m_w x_\alpha b \\ m_w x_\alpha b & m_t \end{bmatrix}\begin{bmatrix} \ddot{\alpha} \\ \ddot{h} \end{bmatrix}+\begin{bmatrix} c_\alpha & 0 \\ 0 & c_h \end{bmatrix}\begin{bmatrix} \dot{\alpha} \\ \dot{h} \end{bmatrix} + \begin{bmatrix} k_\alpha(\alpha) & 0 \\ 0 & k_h \end{bmatrix}\begin{bmatrix} \alpha \\ h \end{bmatrix}=\begin{bmatrix} M \\ -L \end{bmatrix} . \quad (2.1)$$

Where

$$L=\rho U^2 b c_{l_\alpha} s_p\left[\alpha+(\dot{h}/U+(\frac{1}{2}-a)b(\alpha/U))\right] , \quad (2.2)$$

$$+\rho U^2 b c_{l_\beta} s_p \beta+\rho U^2 b c_{l_\gamma} s_p \gamma$$

$$M=\rho U^2 b^2 c_{m_{\alpha-eff}} s_p \left[\alpha+(\dot{h}/U+(\frac{1}{2}-a)b(\alpha/U))\right] , \quad (2.3)$$

$$+\rho U^2 b^2 c_{m_{\beta-eff}} s_p \beta+\rho U^2 b^2 c_{m_{\gamma-eff}} s_p \gamma$$

$$\begin{aligned} c_{m_{\alpha-eff}} &= (\frac{1}{2}+a)c_{l_\alpha}+2c_{m_\alpha} \\ c_{m_{\beta-eff}} &= (\frac{1}{2}+a)c_{l_\beta}+2c_{m_\beta} \\ c_{m_{\gamma-eff}} &= (\frac{1}{2}+a)c_{l_\gamma}+2c_{m_\alpha} \end{aligned} . \quad (2.4)$$

In this study, it is assumed that the spring term $\alpha \cdot k_\alpha(\alpha)$ is nonlinear; a hard spring in fact, is defined as

$$\alpha \cdot k_\alpha(\alpha)=k_1\alpha+k_2\alpha^3 . \quad (2.5)$$

In the case of a symmetric wing structure, that is, $c_{m_\alpha}=0$, it is a model validated experimentally, applicable to a low frequency, subsonic flight case. In this section, the nonlinearity of an aeroelastic system is detailed. To begin with, its dynamics is revealed by numeric simulation, and for convenience sake, defining $c_1=\rho U^2 b s_p$ and $c_2=\rho U^2 b^2 s_p$, the lift term in Eq. (2.2) and moment term in Eq. (2.3) are rewritten as

$$\begin{aligned} L &= c_1 c_{l\alpha}\left[\alpha+(\dot{h}/U+(\frac{1}{2}-a)b(\alpha/U))\right]+c_1 c_{l\beta}\beta+c_1 c_{l\gamma}\gamma \\ M &= c_2 c_{m_{\alpha-eff}}\left[\alpha+(\dot{h}/U+(\frac{1}{2}-a)b(\alpha/U))\right]+c_2 c_{m_{\beta-eff}}\beta+c_2 c_{m_{\gamma-eff}}\gamma \end{aligned} \quad (2.6)$$

Selecting the state variables as $x_1=\alpha, x_2=\dot{\alpha}$, $x_3=h, x_4=\dot{h}$ the dynamic equation can be converted into a state space form as

$$\begin{aligned} \dot{x}_1 &= x_2 \\ \dot{x}_2 &= c_{\alpha_1}x_1+c_{\alpha_{non1}}x_1^3+c_{\dot{\alpha}_1}x_2+c_{h_1}x_3+c_{\dot{h}_1}x_4+c_{\beta_1}\beta+c_{\gamma_1}\gamma \\ \dot{x}_3 &= x_4 \\ \dot{x}_4 &= c_{\alpha_2}x_1+c_{\alpha_{non2}}x_1^3+c_{\dot{\alpha}_2}x_2+c_{h_2}x_3+c_{\dot{h}_2}x_4+c_{\beta_2}\beta+c_{\gamma_2}\gamma \end{aligned} \quad (2.7)$$

where the parameters are defined in the follows.

$$c_{\alpha_1} = c_2 m_t c_{m_{\alpha-eff}} + c_1 m_w x_\alpha b c_{l_\alpha} - m_t k_1, \qquad c_{\alpha_{non1}} = -m_t k_2$$

$$c_{\dot{\alpha}_1} = c_2 m_t c_{m_{\alpha-eff}} (\frac{1}{2} - a) b(1/U) + c_1 m_w x_\alpha b c_{l_\alpha}$$

$$(\frac{1}{2} - a) b(1/U) - c_\alpha m_t \qquad c_{h_1} = k_h m_w x_\alpha b$$

$$c_{\dot{h}_1} = c_2 m_t c_{m_{\alpha-eff}} (1/U) + c_1 m_w x_\alpha b c_{l_\alpha} (1/U) + c_h m_w x_\alpha b$$

$$c_{\beta_1} = c_2 m_t c_{m_{\beta-eff}} + c_1 m_w x_\alpha b c_{l_\beta} \qquad c_{\gamma_1} = c_2 m_t c_{m_{\gamma-eff}} + c_1 m_w x_\alpha b c_{l_\gamma}$$

$$c_{\alpha_2} = -c_2 m_w x_\alpha b c_{m_{\alpha-eff}} - c_1 I_\alpha c_{l_\alpha} + m_w x_\alpha b k_1$$

$$c_{\alpha_{non2}} = m_w x_\alpha b k_2$$

$$c_{\dot{\alpha}_2} = -c_2 m_w x_\alpha b c_{m_{\alpha-eff}} (\frac{1}{2} - a) b(1/U) - c_1 I_\alpha c_{l_\alpha} (\frac{1}{2} - a) b(1/U) + c_\alpha m_w x_\alpha b$$

$$c_{h_2} = -k_h I_\alpha$$

$$c_{\dot{h}_2} = -c_2 m_w x_\alpha b c_{m_{\alpha-eff}} (1/U) - c_1 I_\alpha c_{l_\alpha} (1/U) - c_h I_\alpha$$

$$c_{\beta_2} = -c_2 m_w x_\alpha b c_{m_{\beta-eff}} - c_1 I_\alpha c_{l_\beta}$$

$$c_{\gamma_2} = -c_2 m_w x_\alpha b c_{m_{\gamma-eff}} - c_1 I_\alpha c_{l_\gamma}$$

When the initial condition $x(0) = [h \quad \alpha \quad \dot{h} \quad \dot{\alpha}]$ $= [0.02\text{m} \quad 10\text{degree} \quad 0\text{m/s} \quad 0\text{degree/s}]$ is given and the flight speed U is choose as $19.0625(m/s)$, the simulated parameters are selected in Table 2.1 and the numerical simulation results are shown in Fig. 2.2

As referred to in the preceding section, it then follows form the simulations that a bounded limit cycle oscillation, referred to as the flutter phenomenon, will induce a structural fatigue or deterioration of the flight response in the long run, though a short term effect does cause little damage to the wing structure. The wing is simulated to demonstrate a repeated flutter of invariant amplitude, leading to a need to design a controller as a means to obviate the likely damage to the wing structure. An aeroelastic state space representation, as previously expressed in Eq. (2.7), requires the angles β and γ, against the trailing and leading edges respectively, as the control inputs for the suppression purpose of the wing flutter. That is, the plunge displacement as well as the pitch angle is made converge from the initial conditions toward the origin, that is

$$x = \begin{bmatrix} \alpha \\ h \end{bmatrix} \rightarrow \begin{bmatrix} 0 \\ 0 \end{bmatrix} = x_d \qquad (2.8)$$

Table 2.1. Simulation parameters for an aeroelastic system.

0.6719	c_{m_γ}	-0.1005
.1905m	I_α	$(m_w x_\alpha^2 b^2 + 0.009039)\text{kg}\cdot\text{m}^2$
.036kg.m^2/s	$k_\alpha(\alpha)$	$12.77 + 1003\alpha^2$
7.43kg/s	k_h	2844.4 N/m
.757	m_t	15.57 kg
.358	m_w	4.34kg
0.1566	s_p	0.5945m
	x_α	-(0.0998+a)
0.6719	ρ	1.225kg/m^3

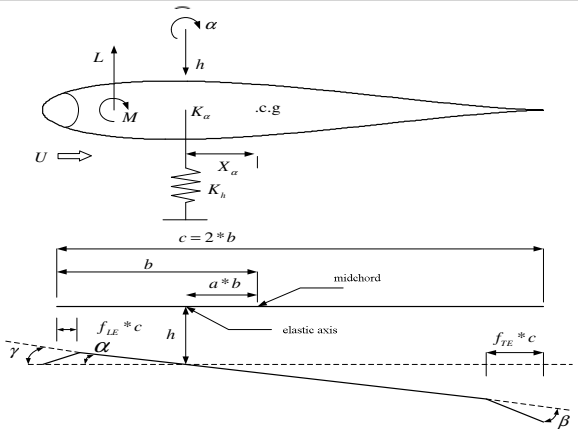

Fig. 2.1. An aeroelastic system model with two freedoms, the plunge displacement and the pitch angle.

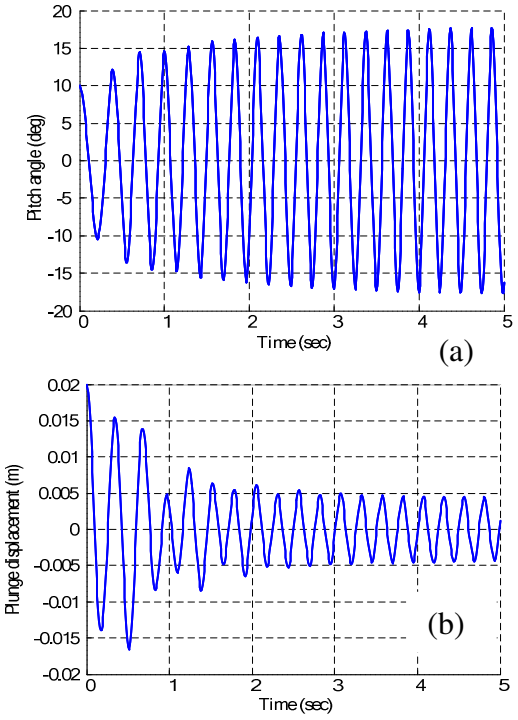

Fig. 2.2. Open loop responses of an aeroelastic system; (a) Time response of the pitch angle. (b) Time response of the plunge displacement.

3. DSMC design

In the case of a sliding mode control, there exists a task of greatest difficulty in practice, that is, a phenomenon of chattering likely accompanied with the control input signal. A concept of boundary layers, proposed by Burton [16], is adopted as a conventional way to rid the control input of the chattering problem at the cost of accuracy, an approach not applicable to meeting high accuracy requirement. This is due to the fact that a higher level of noise may still remain in the control input in particular at a high frequency domain even with the boundary layer design technique.

As illustrated in Fig. 3.1, a dynamic sliding mode control (DSMC) is newly proposed by Bartolinini as an effective manner to eliminate the flutter problem. Incorporating an integrator in the front end, the original system turns into an augmented system with the derivative $w = \dot{u}$ of the original control input as the system input. As a consequence of high frequency noise filtered out of the input w by this integrator, essentially as a low pass filter, unlike the original system, the true system input $u = \int w\,dt$ is gained effectively to remove the flutter occurrence. Hence, the use of a DSMC is of a double advantage of eliminating flutter problem and maintaining the system accuracy. In addition, the high frequency component of external disturbance existing in w is filtered out, for which the disturbance effect is remarkably reduced.

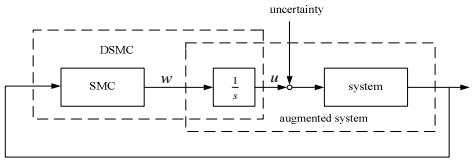

Fig. 3.1. The schematic of a dynamic sliding mode control (DSMC) system.

4. Application of DSMC to aeroelastic systems

It is intended that an application of the DSMC idea, as referred to previously, to an aeroelastic system yields a specified response clear of the flutter problem. The aeroelastic system state space is represented as Eq. (2.7). For the sake of the following design brevity, define

$$u_1 = c_{\beta_1}\beta + c_{\gamma_1}\gamma \text{、} \quad u_2 = c_{\beta_2}\beta + c_{\gamma_2}\gamma, \tag{4.1}$$

$$\begin{aligned} f_1(x_1,x_2,x_3,x_4) &= c_{\alpha_1}x_1 + c_{\alpha_{non1}}x_1^{\,3} \\ &+ c_{\dot{\alpha}_1}x_2 + c_{h_1}x_3 + c_{\dot{h}_1}x_4 \\ f_2(x_1,x_2,x_3,x_4) &= c_{\alpha_2}x_1 + c_{\alpha_{non2}}x_1^{\,3} \\ &+ c_{\dot{\alpha}_2}x_2 + c_{h_2}x_3 + c_{\dot{h}_2}x_4 \end{aligned} \tag{4.2}$$

By way of a change of variables, Eq. (2.7) is turned into

$$\begin{aligned} \dot{x}_1 &= x_2 \\ \dot{x}_2 &= f_1(x_1,x_2,x_3,x_4) + u_1 \\ \dot{x}_3 &= x_4 \\ \dot{x}_4 &= f_2(x_1,x_2,x_3,x_4) + u_2 \end{aligned}$$

Through the idea of DSMC, the differentiation of the original control inputs u_1, u_2 results in the control states $w_1 = \dot{u}_1$, $w_2 = \dot{u}_2$, and then the augmented system is formulated as

$$\begin{bmatrix} \dot{x}_1 \\ \dot{x}_2 \\ \dot{x}_3 \\ \dot{x}_4 \\ \dot{u}_1 \\ \dot{u}_2 \end{bmatrix} = \begin{bmatrix} x_2 \\ f_1(x_1,x_2,x_3,x_4)+u_1 \\ x_4 \\ f_2(x_1,x_2,x_3,x_4)+u_2 \\ 0 \\ 0 \end{bmatrix} + \begin{bmatrix} 0 & 0 \\ 0 & 0 \\ 0 & 0 \\ 0 & 0 \\ 1 & 0 \\ 0 & 1 \end{bmatrix} \begin{bmatrix} w_1 \\ w_2 \end{bmatrix} \tag{4.4}$$

Equation (4.4) can be separated into two parts, i.e.

$$\begin{aligned} \dot{x}_1 &= x_2 \\ \dot{x}_2 &= f_1(x_1,x_2,x_3,x_4) + u_1 \\ \dot{x}_3 &= x_4 \\ \dot{x}_4 &= f_2(x_1,x_2,x_3,x_4) + u_2 \end{aligned} \tag{4.5a}$$

$$\begin{aligned} \dot{u}_1 &= w_1 \\ \dot{u}_2 &= w_2 \end{aligned} \tag{4.5b}$$

An insight into Eqs. (4.5a) and (4.5b) reveals that w_1, w_2 are two variables merely appearing in Eq. (4.5b), which can be fully replaced with $\dot{s}\,|_{u=u_{eq}} = 0$ in the sliding mode according to the equivalent control analysis, a fact irrespective of the system stability. Therefore, when designing a sliding vector, it merely takes Eq. (4.5a) into account, with the system states $\{x_1, x_2, x_3, x_4\}$, and the control inputs u_1, u_2. For the purpose of stabilizing Eq. (4.5a), both u_1 and u_2 are defined as

$$\begin{aligned} u_1 &= -f_1(x_1,x_2,x_3,x_4) - \delta_1 x_1 - \delta_2 x_2 \\ u_2 &= -f_2(x_1,x_2,x_3,x_4) - \delta_3 x_3 - \delta_4 x_4 \end{aligned} \tag{4.6}$$

where δ_1, δ_2, δ_3, δ_4, denoting positive numbers, make Eq. (4.5a) stable, represented as

$$\begin{aligned} \dot{x}_1 &= x_2 \\ \dot{x}_2 &= -k_1 x_1 - k_2 x_2 \\ \dot{x}_3 &= x_4 \\ \dot{x}_4 &= -k_3 x_3 - k_4 x_4 \end{aligned} \tag{4.7}$$

where δ_1, δ_2, δ_3, δ_4 are made according to the specified characteristic roots to meet the system performance requirement. Then sliding vectors s_1, s_2 are selected as

$$\begin{aligned} s_1 &= u_1 + f_1(x_1, x_2, x_3, x_4) + \delta_1 x_1 + \delta_2 x_2 \\ s_2 &= u_2 + f_2(x_1, x_2, x_3, x_4) + \delta_4 x_4 + \delta_3 x_3 \end{aligned} \quad (4.8)$$

It can be clearly seen that as long as the sliding modes $s_1 = 0$, $s_2 = 0$ are satisfied, Eq. (4.6) holds true. By use of a system representation of the sliding modes $s_1 = 0$, $s_2 = 0$, Eq. (4.5b) and the equivalent control principle $\dot{s}\,|_{u=u_{eq}} = 0$, equivalent controls w_{1eq}, w_{2eq} are expressed as

$$\begin{aligned} w_{1eq} &= -\dot{f}_1(x_1, x_2, x_3, x_4) - \delta_1 \dot{x}_1 - \delta_2 \dot{x}_2 \\ &= -[c_{\alpha_1} x_2 + 3c_{\alpha_{non1}} x_1^{\,2} x_2 + c_{\dot{\alpha}_1}(f_1 + u_1) \\ &\quad + c_{h_1} x_4 + c_{\dot{h}_1}(f_2 + u_2)] \\ &\quad - \delta_1 x_2 - \delta_2 (f_1 + u_1) \end{aligned} \quad (4.9)$$

$$\begin{aligned} w_{2eq} &= -\dot{f}_2(x_1, x_2, x_3, x_4) - \delta_3 \dot{x}_3 - \delta_4 \dot{x}_4 \\ &= -[c_{\alpha_2} x_2 + 3c_{\alpha_{non2}} x_1^{\,2} x_2 + c_{\alpha_2}(f_1 + u_1) \\ &\quad + c_{h_{21}} x_4 + c_{\dot{h}_2}(f_2 + u_2)] \\ &\quad - \delta_3 x_4 - \delta_4 (f_2 + u_2) \end{aligned} \quad (4.10)$$

For the sake of approaching time reduction, a exponential approaching law as well as constant speed approaching law is employed in a approaching type such that control laws w_1, w_2 are designed as

$$w_1 = w_{1eq} - k_{\exp 1}(s_1) - \xi_1 \operatorname{sgn}(s_1) \quad (4.11)$$

$$w_2 = w_{2eq} - k_{\exp 2}(s_2) - \xi_2 \operatorname{sgn}(s_2) \quad (4.12)$$

where $k_{\exp 1}$, $k_{\exp 2}$ represent the exponential approaching law, and ξ_1, ξ_2 the constant speed approaching law. Choosing a converging time of 4 sec, then the characteristic root is specified as $-1 \pm 0.5i$, corresponding parameters as $\delta_1 = 1.25$, $\delta_2 = 2$, $\delta_3 = 1.25$, $\delta_4 = 2$, exponential approaching law as $k_{\exp 1} = 50$, $k_{\exp 2} = 175$, and constant speed approaching lawas $\xi_1 = 2$, $\xi_2 = 0.1$. The simulation results will be discussed in full in the next section.

5. Simulation results

In this section, the feasibility of the control law design referred to in the preceding section is validated through numerical simulations. The aeroelastic system parameters, as tabulated in Table 2.1, in a terminal sliding control are simulated with the initial conditions $x(0) = [h \quad \alpha \quad \dot{h} \quad \dot{\alpha}] = [0.02\text{m} \quad 10\text{degree} \quad 0\text{m/s} \quad 0\text{degree/s}]$, a flight speed U of $19.0625 m/s$, and with references $h_d = 0$ and $\alpha_d = 0$ respectively.

Shown in Fig. 5.1 are the simulation results of an unconstrained dynamic sliding mode control. It is noted that from Figs. 5.1(a) and (b) that with a choice of the conjugate pair $-1 \pm 0.5i$, as well as a damping ratio of 0.9 roughly, rather than a furious oscillation during the transient state, the pitch angle and the plunge displacement both converge to the origin roughly at Time = 5 sec.

Plotted in Figs. 5.1(e), (f), (g), (h) are the time responses of the controlled trailing, leading edges, the control laws w_1, w_2, respectively. Even though there is a chattering problem for the control law design, the trailing and leading edge angles, as the true inputs to the aeroelastic system, turn smooth through an integrator. Nevertheless, the smooth inputs are still beyond the confinement of ± 25 °, a motivation to make an improvement as follows.

As illustrated in Fig. 5.2, integrated with an input saturation function in the front end, the dynamic sliding controller takes u_1, u_2 as true inputs, subsequent to the integration of the control laws w_1, w_2. Then derived from Eq. (4.1), the leading and trailing edge angles, i.e. γ and β, are applied to the aeroelastic system through the saturation function. Both the control inputs γ, β are indeed the internal states within the augmented system, and will be inevitably altered during the control process, for which the system response can be made as intended by no means. Thus, the control laws w_1, w_2 are modified in a way, as illustrated in Fig. 5.3, rather than altering the internal states γ, β. The modification is stated as follows.

Illustrated in Fig. 5.3 is the way to modify the control laws w_1, w_2, following the introduction of the saturation function. Firstly, $w_1(0)$, $w_2(0)$ are evaluated by Eqs. (4.11) and (4.12), then explicitly discovering $\dot{\beta}(0)$, $\dot{\gamma}(0)$ at t_0 as

$$\begin{bmatrix} c_{\beta_1} & c_{\gamma_1} \\ c_{\beta_2} & c_{\gamma_2} \end{bmatrix} \begin{bmatrix} \dot{\beta} \\ \dot{\gamma} \end{bmatrix} = \begin{bmatrix} w_1 \\ w_2 \end{bmatrix} \quad (5.1)$$

Taking the trailing edge angle β as an example in Fig. 5.3, given $\dot{\beta}(0)$ and $\beta(0) = 0$, $\beta(1)$ is estimated as $\beta(1) = \beta(0) + \dot{\beta}(0) \cdot \Delta t$. In this case, $\beta(1)$ does not exceed the saturation level, i.e. there is no need to

modify $w_1(0)$, $w_2(0)$. In the same manner, the control laws $w_1(1)$, $w_2(1)$ are evaluated, $\dot{\beta}(1)$ as well as $\dot{\gamma}(1)$ is found by Eq. (5.1), and then $\beta(2)=\beta(1)+\dot{\beta}(1)\cdot\Delta t$. In the case of $\beta(2)$ exceeding the threshold, i.e. an over steep slope $\dot{\beta}(1)$, $\dot{\beta}(1)$ is thus modified into $\dot{\beta}(1)_{\text{saturation}}$ saturation.

The idea of the improvement is made brief as follows. In the event that the input angle at the next instant $(t+1)$ exceeds the saturation level, then the slopes $\dot{\gamma}$, $\dot{\beta}$ at the instant t are requested to be modified into $\dot{\gamma}_{\text{saturation}}$, $\dot{\beta}_{\text{saturation}}$, or otherwise stay unchanged. According to the criterion, the control laws w_1, w_2 are given by Eq. (5.1), with which the modification is completed. The simulation results are presented in Fig. 5.4.

As demonstrated in Figs. 5.4(a) and (b), the controlled pitch angle as well as the plunge displacement exhibits a large amplitude of oscillation during the transient state, and the settling time of 5 sec is extended into 7 sec as the effect of the confinement imposed on the inputs. It can be found that from Figs. 5.4(e) and (f) as well that the leading edge angle is confined between $\pm 25^{\circ}$ for 2 sec or so, then converging to zero gradually. Compared with the above mentioned control strategy, the design of the control laws w_1, w_2 , in place of the direct design of the inputs γ, β, induces a degraded transient response attributed to a more unlikely expected system trajectory. However, the goal of the flutter elimination is as intended reached, elevating the feasibility in practical application.

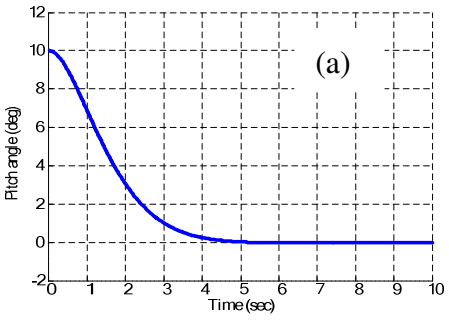

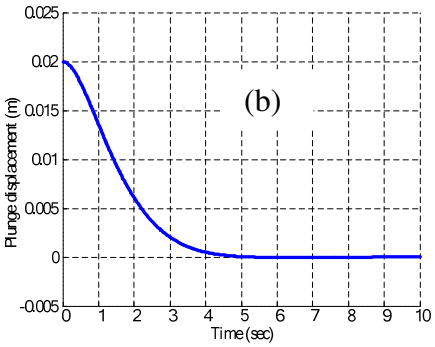

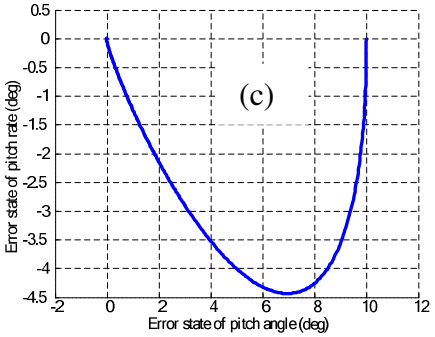

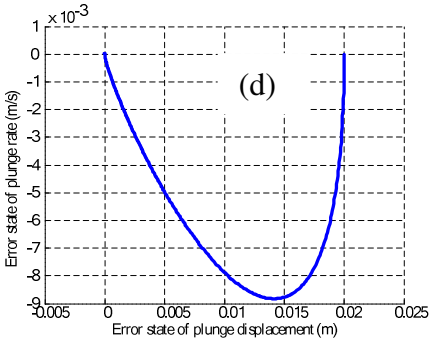

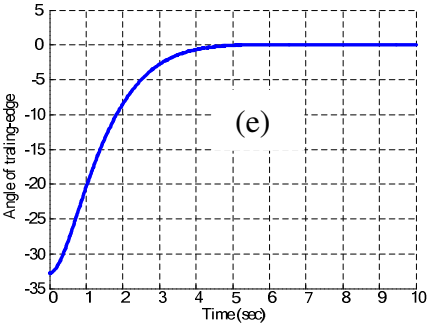

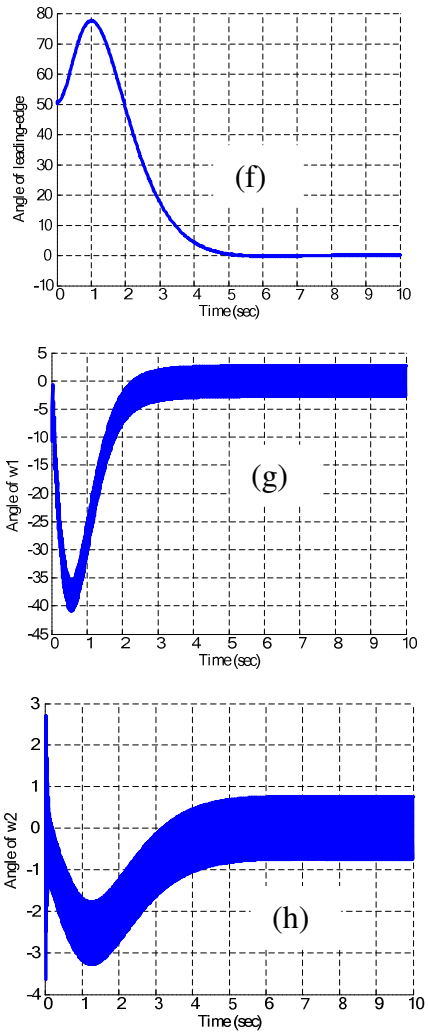

Fig. 5.1. Time responses of an unconstrained wing control in the DSMC. (a) Time response of the pitch angle. (b) Time response of the plunge displacement. (c) Phase plane trajectory of the pitch angle. (d) Phase plane trajectory of the plunge displacement. (e) Time response of the trailing edge angle. (f) Time response of the leading edge angle. (g) Time response of the input w_1. (h) Time response of the input w_2

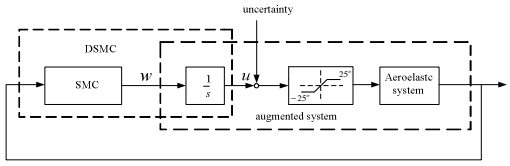

Fig. 5.2. A block diagram of the wing controlled between $[-25^{o}, 25^{o}]$ in a dynamic sliding mode control.

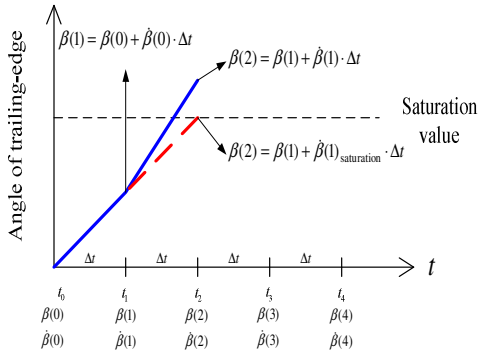

Fig. 5.3. Modification of the trailing edge slope following the introduction of the saturation function.

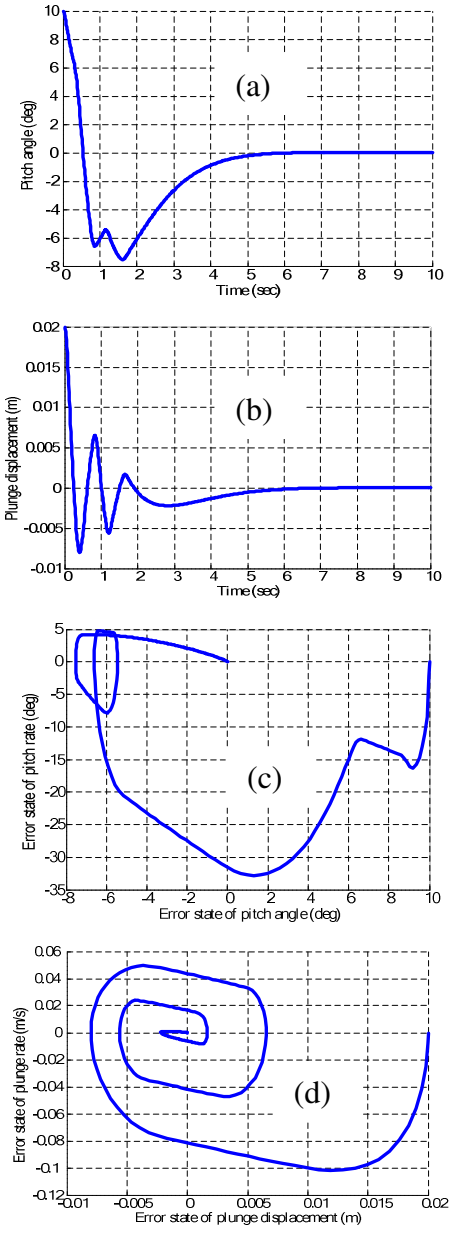

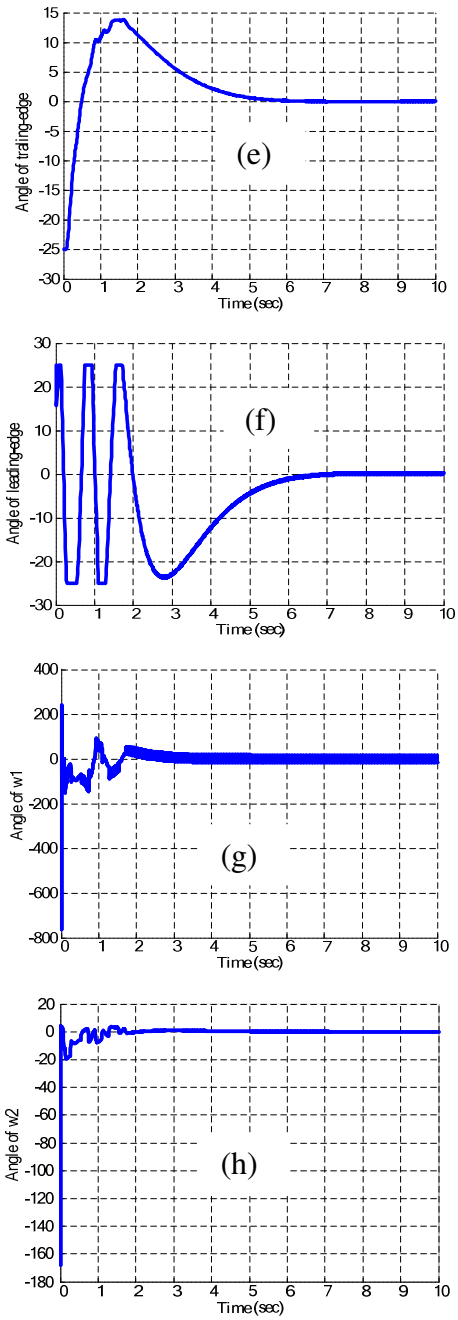

Fig. 5.4. Time responses of a wing constrained between $[-25^{o}, 25^{o}]$ in a dynamic sliding mode control. (a) Time response of the pitch angle. (b) Time response of the plunge displacement. (c) Phase plane trajectory of the pitch angle. (d) Phase plane trajectory of the plunge displacement. (e) Time response of the trailing edge angle. (f) Time response of the leading edge angle. (g) Time response of the input w_1. (h) Time response of the input w_2.

6. Conclusions

This study used both controlled edges as inputs to analysis the performance of an aeroelastic system. Because of a spring with a nonlinear stiffness in an aeroelastic model, a limit cycle oscillation exists, leading to a fatigue in the wing structure as the consequence of a long term vibration with constant amplitude at an invariant frequency. Thus, the DSMC is proposed to suppress the limit cycle oscillation. In terms of a sliding mode control design, the switching between functions remains the biggest annoyance, due to which the chattering is unpleasantly incurred. Proposed in this work, the task is done by directly differentiating the input term in the dynamic sliding mode control. Subsequently, the derivative terms of the inputs are controlled in a sliding mode, and both control law designs are validated by simulations as those being able to effectively reduce chattering and suppress the limit cycle oscillation incurred in wing structures.

Acknowledgements

The financial support of this research by National Science Council, Taiwan, under the grant No. NSC 98-2221-E-006-209-MY2 is greatly appreciated.

Nomenclature

h = the plunge displacement

α = the pitch angle

γ = the angles of the leading edge

β = the angles of the trailing edge

L = lift aerodynamic term

M = moment aerodynamic term

U =the flight speed of the wing

m_t =the total weight of main wing and supporter alike

m_w =the weight of main wing

x_α =the dimensionless distance between the center of mass and the elastic axis

I_α =the moment of inertia

b = the mid-chord

c_α , c_h = the damping coefficients of the pitch angle and the plunge displacement

k_h , $k_{\alpha(\alpha)}$ = the spring stiffness coefficients of the plunge displacement and the pitch angle r

ρ = the air density

a =the dimensionless distance between the elastic axis and the mid-chord

s_p =the Wind Span length

c_{l_α} , c_{m_α} =the lift coefficient and moment coefficient per unit angle of attack

c_{l_β} , c_{m_β} = the lift coefficient and moment coefficient per unit angle of the trailing edge.

c_{l_γ} , c_{m_γ} = the lift coefficient and moment coefficient per unit angle of the leading edge

$c_{m_{\alpha-eff}}$, $c_{m_{\beta-eff}}$, $c_{m_{\gamma-eff}}$ = the moment derivative coefficient for per unit angle of attack, trailing edge and leading edge

References

[1] Lee, B. H. K., LeBlanc, P.: Flutter Analysis of a Two-Dimensional Airfoil with cubic Nonlinear Restoring Force. National Aeronautical Establishment, Aeronautical Note 36, National Reserch Counsil (Canada), 35438, Ottawa, PQ, Canada (1986).

[2] Zhao, L. C., Yang, Z. C.: Chaotic motions of an airfoil with nonlinear stiffness in incompressible flow. Journal of Sound and Vibration, 128(2), 245–254(1990).

[3] Price, S. J., Alighanbari, H., Lee, B. H. K.: The Aeroelastic Response of a Two- dimensional Airfoil with Bilinear and Cubic Nonlinearities. Journal of Fluids and Structure, 9, 175–193(1995).

[4] Kim, S. H., Lee, I.: Aeroelastic Analysis of a Flexible Airfoil with a Freeplay Nonlinearity. Journal of Sound and Vibration, **193**, 823–846(1996).

[5] O"Neill, T., Strganac, T.W.: Aeroelastic Response of a Rigid Wing Supported by Nonlinear Spring. Journal of Aircraft, 35(4), 616–622 (1998).

[6] Lee, B. H. K., Price, S. J., Wong, Y. S.: Nonlinear aeroelastic analysis of airfoils: Bifurcation and chaos. Progress in Aerospace Sciences, **35**, 205–334 (1999).

[7] Singh, S. N., Brenner, M.: Limit Cycle Oscillation and Orbital Stability in Aeroelastic Systems with Torsional Nonlinearity. Nonlinear Dynamics, 31, 435-450(2003).

[8] Strganac, T. W., Ko, J.: Thompson, D. E. Identification and Control of Limit Cycle Oscillations in Aeroelastic Systems. Journal of Guidance, Control, and Dynamics 23(6), 1127-1133(2000).

[9] Bhoir, N.G., Singh, S. N.: Output Feedback Nonlinear Control of an Aeroelastic with Unsteady Aerodynamics. Aerospace Science and Technology 8, 195-205 (2004).

[10] Platanitis, G. Strganac, T. W.: Control of a nonlinear wing section using leading- and trailing-edge surfaces. Journal of Guidance, Control, and Dynamics 27(1), 52-58(2004).

[11] Gujjula, S, Singh, S. N, Yim. W.: Adaptive and Neural Control of a Wing Section Using Leading- and Trailing-edge Surfaces. Aerospace Science and Technology 9, 161-171(2005).

[12] Ko, J., Kurdila, A. J., Strganac, T. W.: Nonlinear Control of a Prototypical Wing Section with Torsional Nonlinearity. Journal of Guidance, Control and Dynamics, **20**(6), 1181–1189(1997).

[13] Block, J., Strganac, T. W.: Applied Active Control for Nonlinear Aeroelastic Structure. Journal of Guidance, Control, and Dynamics, 21, 6, 838-845(1998).

[14] Ko, J., Strganac, T. W., and Kurdila, A. J.: Stability and Control of a Structurally Nonlinear Aeroelastic System. Journal of Guidance, Control, and Dynamics 21(5), 718-725 (1998).

[15] Bhoir, N.G., Singh, S. N.: Control of Unsteady Aeroelastic System via State-Dependent Riccati Equation method. Journal of Guidance, Control, and Dynamics 28(1), 78-84(2005).

[16] Slotine J.E., Li W., Applied nonlinear control, Prentice-Hall, Englewood Cliffs, New Jersey, 1991.

[17] Chen G, Dong X. From chaos to order: methodologies, perspectives and applications. Singapore: World Scientific;1998.

[18] Koshkouei A.J., Burnham K.J. and Zinober A.S.I., Dynamic sliding mode control design, IEE Proc.-Control Theory Appl., Vol. 152, No. 4, pp. 392-396 (2005).

[19] Krupp, D., Shkolnikov, I., and Shtessel, Y., High order sliding modes in dynamic sliding manifolds: SMC design with uncertain actuator. Proceedings of American Control Conference, Chicago, IL, USA, June 28–30, pp. 124–128 (2000).

[20] Theodorsen, T., Garrick, I. E.: Mechanism of flutter: A Theoretical and Experiment Investigation of the Flutter Problem. NACA Rept. 685 (1940).

Chieh-Li Chen

National Cheng Kung University, Taiwan Chieh-Li Chen received the B.S. degree from Department of Mechanical Engineering, National Taiwan University, Taipei, Taiwan, in 1983. Then, he obtained the M.S. and Ph.D. degrees from the University of Manchester Institute of Science and Technology (UMIST), U.K, in 1987 and 1989, respectively, all in control engineering. He is a Professor at the Department of Aeronautics and Astronautics, National Cheng Kung University, Tainan, Taiwan, where he currently teaches in the areas of automatic control and machine vision. His research interests include automation, optimization, nonlinear dynamics, robust control, vibration and energy system management and machine vision.

Chung-Wei Chang

Industrial Technology Research Institute, Taiwan Chung-Wei Chang obtained the B.S. and M.S. degrees from National Cheng Kung University, Tainan, Taiwan, in 2008 and 2010, respectively, all in Department of Aeronautics and Astronautics. In addition, he is an engineer at the Intelligent Machinery Technology Division Mechatronics Control Department, Industrial Technology Research Institute, Taiwan. His research interests include system control, mechatronics and mechanical system design and analysis.

Her Terng Yau

National Chin-Yi University of Technology, Taiwan Her-Terng Yau received the B.S. degree from Department of Mechanical Engineering, National Chung Hsing University, Taichung, Taiwan, in 1994. Then, he obtained the M.S. and Ph.D. degrees from the National Cheng Kung University, Tainan, Taiwan, in 1996 and 2000, respectively, all in mechanical engineering. In addition, he is a Professor at the Department of Electrical Engineering, National Chin-Yi University of Technology, Taichung, Taiwan, where he currently teaches in the areas of automatic control and signal analysis. His research interests include robust control, nonlinear system analysis and control, fuzzy control, and energy system control and management.